

Incomplete Detection of Nonclassical Phase-Space Distributions

M. Bohmann,^{1,*} J. Tiedau,² T. Bartley,² J. Sperling,³ C. Silberhorn,² and W. Vogel¹

¹*Arbeitsgruppe Theoretische Quantenoptik, Institut für Physik, Universität Rostock, D-18051 Rostock, Germany*

²*Integrated Quantum Optics Group, Applied Physics,
University of Paderborn, 33098 Paderborn, Germany*

³*Clarendon Laboratory, University of Oxford, Parks Road, Oxford OX1 3PU, United Kingdom*

(Dated: October 2, 2018)

We implement the direct sampling of negative phase-space functions via unbalanced homodyne measurement using click-counting detectors. The negativities significantly certify nonclassical light in the high-loss regime using a small number of detectors which cannot resolve individual photons. We apply our method to heralded single-photon states and experimentally demonstrate the most significant certification of nonclassicality for only two detection bins. By contrast, the frequently applied Wigner function fails to directly indicate such quantum characteristics for the quantum efficiencies present in our setup without applying additional reconstruction algorithms. Therefore, we realize a robust and reliable approach to characterize nonclassical light in phase space under realistic conditions.

Introduction.— Photons embody the wave-particle dualism—a governing principle of quantum physics—as they represent the elementary particle of electromagnetic waves. They also provide the essential building blocks for scalable quantum technologies [1, 2], and fundamental quantum effects are intertwined with the properties of such particles of light, e.g., antibunching [3] and sub-Poisson photon statistics [4]. For this reason, resource-efficient detection schemes which enable the characterization on the single-photon level are indispensable.

In order to uncover quantum features of a physical system, the concept of phase-space distribution functions has been extended from the classical domain to be applicable in quantum optics. This yields the prominent Wigner function [5] and its s -parametrized generalizations [6], which include the Glauber-Sudarshan P [7, 8] and Husimi Q [9] functions. Based on such quasiprobability distributions, quantum effects can be uniquely identified via negativities within them [10–12]. Thus, since its first applications [13, 14], the reconstruction of the Wigner function became a frequently applied method. This led to remarkable insights into the quantum properties of complex quantum systems, such as reported in Refs. [15–19]. Still, there are limitations to this approach. For example, the directly reconstructed Wigner function of a single photon becomes entirely non-negative when the overall loss exceeds 50% [20]—a challenging bound for many experimental scenarios. In such cases, negativities can be recovered by employing optimized reconstruction algorithms which compensate for losses [21].

In addition, information-complete measurements and data processing algorithms are necessary for a phase-space quantum state reconstruction. For instance, the reconstruction can be based on quadrature [22, 23] or displaced photon-number measurements [24]. The latter can be obtained via unbalanced homodyne detection [24], which has been implemented, e.g., in Refs. [25–27]. However, in many practical scenarios, such optimal

detection schemes are not accessible because of experimental limitations, such as nonunity detection efficiencies and a limited resolution of adjacent photon numbers. In such cases, an inversion from the measured data to the photon-number statistics is required [25–27], which is problematic when employing information-incomplete detection schemes. It is also noteworthy that even a partial state reconstruction can reveal nonclassicality as it was demonstrated for marginal distributions [28].

A more realistic resource is quasi-photon-number-resolving or click-counting detectors [29–34], which discriminate between clicks rather than photocounts. Despite their limitations, a number of vital quantum features can be directly obtained from the recorded click-counting statistics [35–38]. Furthermore, the theory of phase-sensitive measurements with such detectors has been derived [39–41]. Specifically, the click-based counterpart to the unbalanced homodyne detection has been proposed together with a click-based versions of phase-space functions [41]. Yet, an experimental confirmation of this theory is missing to date.

In this Letter, we report on the direct sampling of phase-space functions of heralded single-photon states via unbalanced homodyne detection with time-bin-multiplexed click-counting detectors. The resulting phase-space functions directly show negativities even for quantum efficiencies significantly below 50%. Moreover, this is achieved via a direct sampling of the measured click statistics, which does not require an inversion to the photon-number statistics and is intrinsically robust to losses. We also confirm the theoretical prediction from Ref. [41] that fewer detection bins lead to more significant signatures of nonclassical light. Therefore, we implement a reliable method to access the quantum properties of light for application under realistic conditions.

Click-based phase-space functions.—In unbalanced homodyne detection [24], the quantum light under study is displaced by mixing it on an unbalanced beam split-

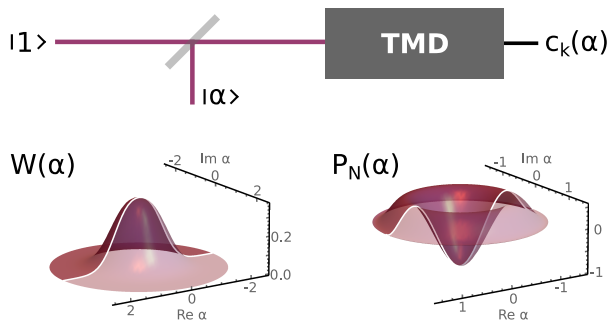


FIG. 1. Top: A signal, e.g., a single photon $|1\rangle$, and a coherent state $|\alpha\rangle$ are superimposed on a highly transmissive beam splitter and measured with a click-counting device, which is in our case a time-bin multiplexing detector (TMD). Bottom: The non-negative Wigner function $W(\alpha)$ for single photon and a detection efficiency of 21% (left) is depicted. In the same scenario, its directly sampled click-counting counterpart (right, $N = 4$) shows clear negativities.

ter with a weak coherent state. The resulting displaced state is then measured with a photon-number-resolving detector. Recently, the theory for such a scheme was generalized to allow for an operation using click-counting devices [41]; see Fig. 1.

In such a scheme, the directly measured click statistics $c_k(\alpha)$ is the probability that k out of the N detection bins record coincidental clicks [42]. Based on this statistics, we obtain—up to a positive normalization constant—the desired phase-space function [41],

$$P_N(\alpha; x) = \sum_{k=0}^N \left(\frac{x-2}{x} \right)^k c_k(\alpha), \quad (1)$$

for any even number N of detection bins (the parameter x is discussed in the next paragraph). In addition, the sampling error is given by

$$[\Delta P_N(\alpha; x)]^2 = \sum_{k=0}^N \left(\frac{x-2}{x} \right)^{2k} \frac{c_k(\alpha) [1 - c_k(\alpha)]}{\omega}, \quad (2)$$

where ω is the number of recorded data points for a given displacement α .

The parameter x in Eq. (1) can be related to s -parametrized phase-space functions [6] ($s \in [-1, 1]$) and the detection efficiency η via $x = \eta(1 - s)$. Let us recall that $s = 0$ defines the Wigner function. As demonstrated in Ref. [41], any negativity in $P_N(\alpha; x)$ for any even N is a sufficient condition for nonclassicality. In the limit of an infinite number of detection bins, $N \rightarrow \infty$, $P_N(\alpha; x)$ approaches the true s -parametrized phase-space function. This then results in a necessary and sufficient nonclassicality characterization. Also note that beyond the specific identification $x = \eta(1 - s)$, an arbitrary nonzero number can be assigned to the parameter x [43].

One of the main benefits of the phase-space distribution Eq. (1) for a finite and even N is that it can

become negative even if its s -parametrized counterpart (without corrections for detection losses) is completely non-negative [41]. To illustrate this, the example of a single photon is shown in Fig. 1 for a quantum efficiency $\eta = 21\%$, which corresponds to our experimental conditions. Clearly, the phase-insensitive Wigner function ($s = 0$) is non-negative. Still, the theory of the click-counting phase-space function for $x|_{s=0} = \eta$ predicts clear negativities, $P_N(0; x) < 0$.

Experimental implementation.—The full experiment was conducted using the setup shown in Fig. 2. This consists of three main parts: generation of heralded single-photon states, interference with a weak coherent beam, and detection on a time-multiplexed detector (TMD). The initial light from a Ti:sapphire oscillator at 80 MHz pumps an optical parametric oscillator (OPO) to generate light at 1550 nm. This pumps a periodically poled lithium niobate (PPLN) crystal to generate second harmonic light (SHG) at 775 nm. This light is split from the residual pump using a dichroic mirror, and then used to pump the source of heralded single photons, namely parametric down-conversion in a periodically poled KTP waveguide. The source is described in detail in Refs. [44, 45]. Prior to the waveguide, the pump is frequency-picked down to 1 MHz. This is required to ensure that there are no overlapping pulses registered by the TMD. The temporal mode of this light is then adjusted using a 4-f line, to ensure the bandwidth of the pump is set to give a spectrally decorrelated down-converted state. Meanwhile, the residual pump from the SHG also undergoes pulse-picking and spectral mode shaping such that it is synchronized and mode matched to the down-conversion. The overlap is 70%, determined from a Hong-Ou-Mandel-type experiment between the heralded single photon and the weak local oscillator. The coherent state amplitude $|\alpha|$ is adjusted with a computer-controlled variable attenuator. The experimental uncertainty in determining $|\alpha|$ ($\sim 20\%$) predominantly arises for temporal drifts in the setup over an experimental run. Following interference, the resulting states are incident on a TMD with a bin separation of 100 ns. Heralding is performed by delaying the herald mode by 400 ns, which is then incident on the other input port of the TMD.

The advantage of time-bin multiplexing is that we only need two detectors, which in our case are superconducting nanowire single-photon detectors, characterized in a previous experiment [46], together with a given number of fiber-loop delays to obtain $N/2$ time bins per detector, which correspond to N physical detectors in the spatial multiplexing configuration [29–31]. Our TMD divides an incident light pulse into up to $N = 8$ time bins per input.

Following interference, one mode is measured by a TMD to provide the click statistics $c_k(\alpha)$. To sample the phase-space function P_N , we record approximately $\omega = 1.4 \times 10^6$ heralded photon states per coherent amplitude for $N = 8$ detection bins. In order to achieve fewer

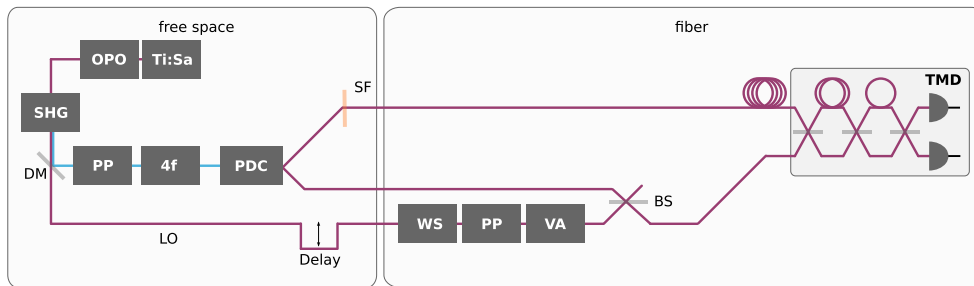


FIG. 2. Schematic experimental setup. A Ti:sapphire laser (Ti:Sa) (down-sampled to 1 MHz) drives an optical parametric oscillator (OPO). The pulsed light is frequency doubled by second harmonic generation (SHG), and the pump is filtered with a dichroic mirror (DM). The SHG pulse undergoes pulse picking (PP) down to 1 MHz, followed by a 4-f (4f) line to set the pulse length, and is used to generate photon pairs in a parametric down-conversion (PDC) process. Before both modes are recorded with time-multiplexed detectors (TMD), one of them is coherently displaced by the local oscillator (LO), mode matched by a time delay, spectral wave shaper (WS) and pulse picker (PP), and attenuated using a variable attenuator (VA), before interfering at an asymmetric beam splitter (BS), with reflection-transmission ratio of 17 : 83.

bins ($N = 2, 4$), we can join several detection bins into clusters [43]. A detailed theoretical model of the state preparation and the measurement is also provided in the Supplemental Material [43].

Direct sampling of phase-space functions.—Applying Eqs. (1) and (2), we can directly sample the phase-space function from our data. Among other imperfections, our model [43] takes unavoidable higher-photon number contributions of the heralded single-photon state into account. Also, impurities originating from the mode mismatching of the signal and LO are considered, which yields a displacement-dependent dark-count rate [40, 43]. Finally, let us stress that our estimated overall detection efficiency, obtained via the fit to our model, is $\eta = 21\%$ —thus, clearly below 50%.

For the four-bin detection ($N = 4$), our rotationally symmetric, sampled phase-space distribution P_N is shown for $x = \eta$ in Fig. 3. The most important observation is that this function shows clear negativities around the origin of phase space, certifying the nonclassical character of the quantum state. Such a negative dip at $|\alpha| = 0$ is typical for single-photon states, cf. Fig. 1. Furthermore, we find a good agreement of the obtained phase-space function with our theoretical model. Note that the estimation of the amplitude $|\alpha|$ of the displacement is challenging because the mean photon number cannot be simply obtained by click-counting devices [42]. More importantly, however, this error does not affect the significance of the certified negativities just their location in phase space.

As mentioned earlier (see also Fig. 1), the overall detection efficiency of the setup does not allow for a direct reconstruction of a negative Wigner function. This would require a postprocessing to refit the data to a lossless scenario [21]. With our technique, such postprocessing becomes superfluous since we directly sample our nonclassical phase-space function according to Eq. (1). In particular, it is sufficient to find one x for which negativ-

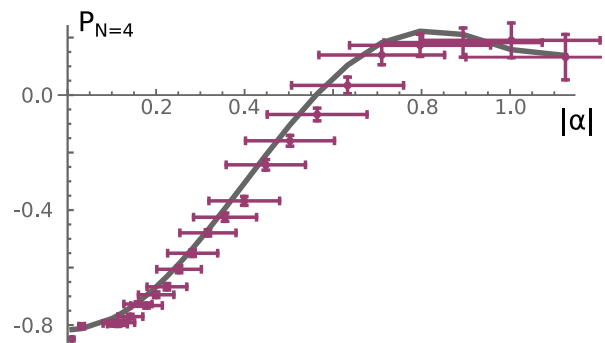


FIG. 3. The pointwise sampled phase-space function $P_N(\alpha; x)$, for $N = 4$ and $x = 0.21$, is shown and compared with the theoretical model (solid curve).

ities become significant. Such an x can be chosen arbitrarily and without prior knowledge about losses. Therefore, our technique is a more direct and robust approach to uncover nonclassical features of light. Moreover, the reconstruction of the Wigner function with unbalanced homodyne detection requires a full photon-number resolution [24]. Again, we demonstrate that such a premise is not required with our alternative approach.

Number-of-bins dependence.—A surprising theoretical finding in Ref. [41] is that fewer detection bins lead to an improved verification of nonclassicality. Let us challenge this statement by comparing our results for different numbers of detection bins.

For this reason, we analyzed the data for two and eight detection bins in addition to the previously studied case, $N = 4$. The correspondingly sampled phase-space functions are shown in Fig. 4 ($x = 0.21$) together with the theoretical model. Again, theory and experiment exhibit good agreement, and in both cases, $N = 8$ and $N = 2$, a negativity at the origin of phase space is present.

To quantitatively assess the quality of the verified nonclassicality, we analyze the signed significance Σ of the

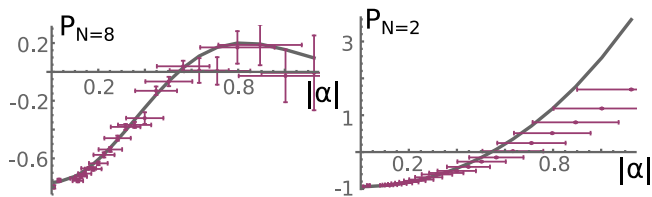


FIG. 4. The sampled phase-space functions and the theoretical models (solid curves) for eight (left) and two (right) detection bins are displayed.

phase-space functions. The signed significance is the ratio of the sampled values and their errors,

$$\Sigma = \frac{P_N(\alpha; x)}{\Delta P_N(\alpha; x)}, \quad (3)$$

cf. Eqs. (1) and (2). This means that for $\Sigma < 0$, we certify the nonclassicality with $|\Sigma|$ standard deviations. In Fig. 5, the signed significances for the different numbers of detectors are plotted as a function of the parameter $x \in [0.10, 0.45]$. We find that the curve for $N = 4$ (dashed) is always below the one for $N = 8$ (solid), and the case $N = 2$ (dotted) is below both. Therefore, we confirm for our data that the verification of nonclassicality is indeed improved by reducing the number of detection bins.

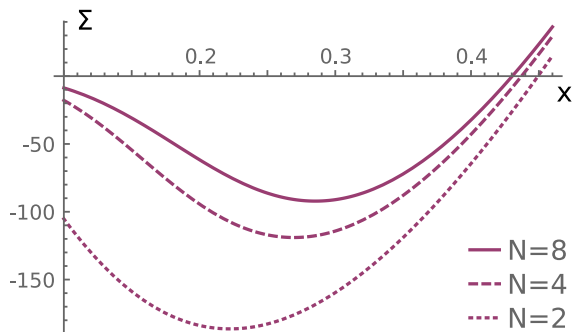


FIG. 5. The signed significance Σ [Eq. (3)] at the origin ($\alpha = 0$) is shown as a function of x .

Furthermore, the maximal verification of nonclassicality with $|\Sigma| = 186$ standard deviations is obtained for two detection bins and $x = 0.22$. This corresponds approximately to the click-counting phase-space distribution related to the Wigner function, where $x = \eta(1 - s)$ and $x|_{s=0} = 0.21$. Surprisingly, the most significant negativities for the four- and eight-bin scenarios are obtained for higher x values, corresponding to phase-space functions closer to the Q function ($s = -1$). However, all distributions eventually become non-negative for larger x values. It is also worth mentioning that $x \rightarrow 0$ corresponds to the often highly singular Glauber-Sudarshan P function ($s = 1$). In this limit, we do not obtain significant negativities from the sampled data, $\Sigma \gtrsim 0$.

Discussion.—Let us briefly compare our technique to other approaches. The advantage of our method is a direct sampling rather than employing challenging optimization algorithms. Thus, it allows one to characterize quantum light in a simple and direct way. Furthermore, our approach works even in the high-loss regime. In particular, it is sufficient to find one x , which we can freely choose without imposing or estimating the overall losses in our setup, such that a negative phase-space distribution is obtained, cf. Fig. 5. Other data processing approaches, e.g., based on balanced homodyne detection, can also correct for losses. Yet, they require precise information about the losses for their operation. Other optimization strategies in data analysis, such as used maximum likelihood approaches, also become superfluous with our technique. Therefore, our sampling method is fast and robust and requires minimal information about the detection scheme.

Conclusions.—We implemented a detection scheme which yields nonclassical phase-space distributions via a direct sampling from the data obtained by an information-incomplete detection system. Our technique renders it possible to certify nonclassical light under realistic conditions even for high losses. Furthermore, sophisticated reconstruction algorithms become superfluous. The application to a heralded single-photon state in the presence of high losses also confirms the theoretical prediction that fewer detection bins can be even advantageous for the verification of quantum light.

Our technique resembles an unbalanced homodyne detection scheme which, however, uses widely accessible click-counting devices instead of photon-number-resolving detectors. The measured click-counting distribution is used to sample our desired function by scanning over the phase space, which is achieved by adjusting the local oscillator. Our click-counting device is a time-bin multiplexing detector which allows us to resolve up to eight bins measured with two detectors. This equals eight physical detectors when compared to other multiplexing approaches.

Using a parametric down-conversion source, we produced single-photon states, and a theoretical model was developed. Our analysis showed that we operate in a comparably high-loss regime, for which other methods would require loss corrections in order to exhibit the nonclassicality. Here, however, we have been able to uncover nonclassical light with high statistical significance via direct sampling. This shows that imperfect measurement can offer highly sensitive nonclassicality tests, even compared to perfect photon-number-resolving detectors.

Beyond our proof-of-concept demonstration for phase-symmetric single-photon states, our technique can be applied to arbitrary quantum light and straightforwardly generalized to multimode scenarios. Because of its simplicity and reliability, our method has the potential to find many applications in quantum optics and quan-

tum technology, which require sturdy components and directly accessible methods. Therefore, we realized a technique which provides a practical tool for the characterization of nonclassical light in phase space.

Acknowledgements.—M.B. gratefully acknowledges financial support by the Deutsche Forschungsgemeinschaft through Grant No. VO 501/22-2. J.T., J.S., C.S., and W.V. acknowledge funding from the European Union’s Horizon 2020 research and innovation programme under Grant No. 665148 (QCUMbER). C.S. acknowledges funding from the Gottfried Wilhelm Leibniz-Preis. T.B. acknowledges financial support from the DFG (Deutsche Forschungsgemeinschaft) under SFB/TRR 142.

* martin.bohmann@uni-rostock.de

- [1] T. E. Northup and R. Blatt, Quantum information transfer using photons, *Nat. Photon.* **8**, 356 (2014).
- [2] A. F. Koenderink, A. Alù, and A. Polman, Nanophotonics: Shrinking light-based technology, *Science* **348**, 516 (2015).
- [3] H. J. Kimble, M. Dagenais, and L. Mandel, Photon Antibunching in Resonance Fluorescence, *Phys. Rev. Lett.* **39**, 691 (1977).
- [4] R. Short and L. Mandel, Observation of Sub-Poissonian Photon Statistics, *Phys. Rev. Lett.* **51**, 384 (1983).
- [5] E. Wigner, On the Quantum Correction For Thermodynamic Equilibrium, *Phys. Rev.* **40**, 749 (1932).
- [6] K. E. Cahill and R. J. Glauber, Density Operators and Quasiprobability Distributions, *Phys. Rev.* **177**, 1882 (1969).
- [7] R. J. Glauber, Coherent and Incoherent States of the Radiation Field, *Phys. Rev.* **131**, 2766 (1963).
- [8] E. C. G. Sudarshan, Equivalence of Semiclassical and Quantum Mechanical Descriptions of Statistical Light Beams, *Phys. Rev. Lett.* **10**, 277 (1963).
- [9] K. Husimi, Some formal properties of the density matrix, *Proc. Phys. Math. Soc. Jpn.* **22**, 264 (1940).
- [10] U. M. Titulaer and R. J. Glauber, Correlation functions for coherent fields, *Phys. Rev.* **140**, B676 (1965).
- [11] R. L. Hudson, When is the Wigner quasi-probability density non-negative?, *Rep. Math. Phys.* **6**, 249 (1974).
- [12] L. Mandel, Non-classical states of the electromagnetic field, *Phys. Scr. T* **12**, 34 (1986).
- [13] D. T. Smithey, M. Beck, M. G. Raymer, and A. Faridani, Measurement of the Wigner distribution and the density matrix of a light mode using optical homodyne tomography: Application to squeezed states and the vacuum, *Phys. Rev. Lett.* **70**, 1244 (1993).
- [14] D. Leibfried, D. M. Meekhof, B. E. King, C. Monroe, W. M. Itano, and D. J. Wineland, Experimental Determination of the Motional Quantum State of a Trapped Atom, *Phys. Rev. Lett.* **77**, 4281 (1996).
- [15] S. Deléglise, I. Dotsenko, C. Sayrin, J. Bernu, M. Brune, J.-M. Raimond, and S. Haroche, Reconstruction of nonclassical cavity field states with snapshots of their decoherence, *Nature (London)* **455**, 510 (2008).
- [16] B. Vlastakis, G. Kirchmair, Z. Leghtas, S. E. Nigg, L. Frunzio, S. M. Girvin, M. Mirrahimi, M. H. Devoret, R. J. Schoelkopf, Deterministically Encoding Quantum Information Using 100-Photon Schrödinger Cat States, *Science* **342**, 607 (2013).
- [17] O. Morin, K. Huang, J. Liu, H. Le Jeannic, C. Fabre, and J. Laurat, Remote creation of hybrid entanglement between particle-like and wave-like optical qubits, *Nat. Photon.* **8**, 570 (2014).
- [18] C. Wang *et al.*, A Schrödinger cat living in two boxes, *Science* **352**, 1087 (2016).
- [19] D. V. Sychev, A. E. Ulanov, A. A. Pushkina, M. W. Richards, I. A. Fedorov, and A. I. Lvovsky, Enlargement of optical Schrödinger’s cat states, *Nat. Photon.* **11**, 379 (2017).
- [20] A. I. Lvovsky, H. Hansen, T. Aichele, O. Benson, J. Mlynek, and S. Schiller, Quantum State Reconstruction of the Single-Photon Fock State, *Phys. Rev. Lett.* **87**, 050402 (2001).
- [21] A. I. Lvovsky, Iterative maximum-likelihood reconstruction in quantum homodyne tomography, *J. Opt. B* **6**, S556 (2004).
- [22] W. Vogel and D.-G. Welsch, *Quantum Optics* (Wiley-VCH, Weinheim, 2006).
- [23] A. I. Lvovsky and M. G. Raymer, Continuous-variable optical quantum-state tomography, *Rev. Mod. Phys.* **81**, 299 (2009).
- [24] S. Wallentowitz and W. Vogel, Unbalanced homodyning for quantum state measurements, *Phys. Rev. A* **53**, 4528 (1996).
- [25] K. Banaszek, C. Radzewicz, K. Wódkiewicz, and J. S. Krasinski, Direct measurement of the Wigner function by photon counting, *Phys. Rev. A* **60**, 674 (1999).
- [26] K. Laiho, Katiúscia N. Cassemiro, D. Gross, and C. Silberhorn, Probing the Negative Wigner Function of a Pulsed Single Photon Point by Point, *Phys. Rev. Lett.* **105**, 253603 (2010).
- [27] G. Donati, T. J. Bartley, X.-M. Jin, M.-D. Vidrighin, A. Datta, M. Barbieri, and I. A. Walmsley, Observing optical coherence across Fock layers with weak-field homodyne detectors, *Nat. Commun.* **5**, 5584 (2014).
- [28] J. Park, Y. Lu, J. Lee, Y. Shen, K. Zhang, S. Zhang, M. S. Zubairy, K. Kim, and H. Nha, Revealing nonclassicality beyond Gaussian states via a single marginal distribution, *Proc. Natl. Acad. Sci. U.S.A.* **114**, 891 (2017).
- [29] J. Řeháček, Z. Hradil, O. Haderka, J. Peřina Jr., and M. Hamar, Multiple-photon resolving fiber-loop detector, *Phys. Rev. A* **67**, 061801(R) (2003).
- [30] M. J. Fitch, B. C. Jacobs, T. B. Pittman, and J. D. Franston, Photon-number resolution using time-multiplexed single-photon detectors, *Phys. Rev. A* **68**, 043814 (2003).
- [31] D. Achilles, C. Silberhorn, C. Śliwa, K. Banaszek, and I. A. Walmsley, Fiber-assisted detection with photon number resolution, *Opt. Lett.* **28**, 2387 (2003).
- [32] V. Schettini, S. V. Polyakov, I. P. Degiovanni, G. Brida, S. Castelletto, and A. L. Migdall, Implementing a multiplexed system of detectors for higher photon counting rates, *IEEE J. Sel. Top. Quantum Electron.* **13**, 978 (2007).
- [33] J. S. Lundeen, A. Feito, H. Coldenstrodt-Ronge, K. L. Pagnell, C. Silberhorn, T. C. Ralph, J. Eisert, M. B. Plenio, and I. A. Walmsley, Tomography of quantum detectors, *Nat. Phys.* **5**, 27 (2009).
- [34] J. C. F. Matthews, X.-Q. Zhou, H. Cable, P. J. Shadbolt, D. J. Saunders, G. A. Durkin, G. J. Pryde, and J. L. O’Brien, Towards practical quantum metrology with

- photon counting, *npj Quantum Inf.* **2**, 16023 (2016).
- [35] T. J. Bartley, G. Donati, X.-M. Jin, A. Datta, M. Barbieri, and I. A. Walmsley, Direct Observation of Sub-Binomial Light, *Phys. Rev. Lett.* **110**, 173602 (2013).
- [36] J. Sperling, M. Bohmann, W. Vogel, G. Harder, B. Brecht, V. Ansari, and C. Silberhorn, Uncovering Quantum Correlations with Time-Multiplexed Click Detection, *Phys. Rev. Lett.* **115**, 023601 (2015).
- [37] J. Sperling, T. J. Bartley, G. Donati, M. Barbieri, X.-M. Jin, A. Datta, W. Vogel, and I. A. Walmsley, Quantum Correlations from the Conditional Statistics of Incomplete Data, *Phys. Rev. Lett.* **117**, 083601 (2016).
- [38] M. Bohmann, R. Kruse, J. Sperling, C. Silberhorn, and W. Vogel, Probing free-space quantum channels with laboratory-based experiments, *Phys. Rev. A* **95**, 063801 (2017).
- [39] J. Sperling, W. Vogel, and G. S. Agarwal, Balanced homodyne detection with on-off detector systems: Observable nonclassicality criteria, *Europhys. Lett.* **109**, 34001 (2015).
- [40] T. Lipfert, J. Sperling, and W. Vogel, Homodyne detection with on-off detector systems, *Phys. Rev. A* **92**, 053835 (2015).
- [41] A. Luis, J. Sperling, and W. Vogel, Nonclassicality Phase-Space Functions: More Insight with Fewer Detectors, *Phys. Rev. Lett.* **114**, 103602 (2015).
- [42] J. Sperling, W. Vogel, and G. S. Agarwal, True photocounting statistics of multiple on-off detectors, *Phys. Rev. A* **85**, 023820 (2012).
- [43] See Supplemental Material, which includes Refs. [40–42, 46–48], for additional information about the theoretical model and the data analysis.
- [44] A. Eckstein, A. Christ, P. J. Mosley, and C. Silberhorn, Highly efficient single-pass source of pulsed single-mode twin beams of light, *Phys. Rev. Lett.* **106**, 013603 (2011).
- [45] G. Harder, V. Ansari, B. Brecht, Benjamin, T. Dirmeier, C. Marquardt, and C. Silberhorn, An optimized photon pair source for quantum circuits, *Opt. Express* **21**, 12 (2013).
- [46] M. Bohmann, R. Kruse, J. Sperling, C. Silberhorn, and W. Vogel, Direct calibration of click-counting detectors, *Phys. Rev. A* **95**, 033806 (2017).
- [47] J. Sperling, W. Vogel, and G. S. Agarwal, Quantum state engineering by click counting, *Phys. Rev. A* **89**, 043829 (2014).
- [48] F. M. Miatto, A. Safari, and R. W. Boyd, Theory of multiplexed photon number discrimination, [arXiv:1601.05831](https://arxiv.org/abs/1601.05831).

Supplemental Material: Incomplete Detection of Nonclassical Phase-Space Distributions

M. Bohmann,^{1,*} J. Tiedau,² T. Bartley,² J. Sperling,³ C. Silberhorn,² and W. Vogel¹

¹*Arbeitsgruppe Theoretische Quantenoptik, Institut für Physik, Universität Rostock, D-18051 Rostock, Germany*

²*Integrated Quantum Optics Group, Applied Physics,
University of Paderborn, 33098 Paderborn, Germany*

³*Clarendon Laboratory, University of Oxford, Parks Road, Oxford OX1 3PU, United Kingdom*

This supplemental material provides additional details about the theory and the experiment. In Sec. I, the click-counting theory is presented and our detectors are characterized. In Sec. II, we formulate the model of the heralded single-photon state including imperfections.

I. DETECTION THEORY

A. Detector response

The theory of click-counting detectors, i.e., multiplexing layouts with on-off detectors, was established in Ref. [1] and generalized to interferometric setups in Ref. [2]. For our scenario of unbalanced homodyne detection, it takes the form [3]

$$c_k(\alpha) = \left\langle : \binom{N}{k} (e^{-\hat{\Gamma}})^{N-k} (\hat{1} - e^{-\hat{\Gamma}})^k : \right\rangle_{\hat{\rho}_\alpha}, \quad (1)$$

where \dots indicates the normal-ordering prescription and $\hat{\Gamma}$ is the detector response function. The averaging is performed using the displaced quantum state $\hat{\rho}_\alpha = \hat{D}(-\alpha)\hat{\rho}\hat{D}^\dagger(-\alpha)$, with $\hat{D}(\alpha)$ denoting the displacement operator.

We can use calibration techniques to determine the properties of our detection system [4]. Here, this allows us to write the detector response function as

$$\hat{\Gamma} = \frac{\eta}{N}\hat{n} + \nu(\alpha), \quad (2)$$

where \hat{n} is the photon-number operator and $\nu(\alpha)$ is a displacement-dependent dark-count rate. The latter models the mode mismatch between the signal and the coherent state, i.e., local oscillator [2].

In our analysis, all losses in the setup are combined into one quantum efficiency η . A best fit of the data with the model in Sec. II yields an overall detection efficiency of the setup of $\eta = 21\%$. Further, $\nu(\alpha)$ is a linear function of the displacement $|\alpha|^2$, $\nu(\alpha) = \mu\eta|\alpha|^2/N$ [2]. We estimate a mode mismatch of 30% between the signal state and the coherent state, $0.3/0.7 \approx 0.43 = \mu$. See also Fig. 1.

B. Clustering of detection bins

In our initial measurement configuration, we have eight detection bins. We now demonstrate how this allows us

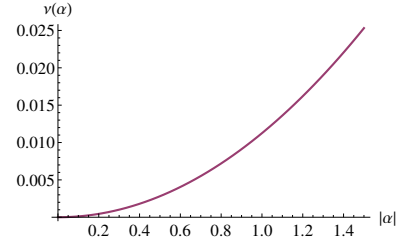


FIG. 1. The experimentally estimated dependence of the dark-count rate $\nu(\alpha)$ on the coherent displacement $|\alpha|$ to account for mode mismatch for $\eta = 0.21$ and $N = 8$.

to infer the outcomes for four and two detection bins. This method, called *clustering*, is based on a similar derivation as considered for the click counting statistics [1]. In general, we measure a coincidence statistics

$$c_{k_1, \dots, k_N} = \left\langle : \prod_{j=1}^N \left(\left[e^{-\eta(\hat{n} + \mu|\alpha|^2)/N} \right]^{1-k_j} \right. \right. \\ \left. \left. \times \left[\hat{1} - e^{-\eta(\hat{n} + \mu|\alpha|^2)/N} \right]^{k_j} \right) : \right\rangle_{\hat{\rho}_\alpha}, \quad (3)$$

where $k_j = 0$ and $k_j = 1$ means that no click one and one click was recorded in the j th detection bin, respectively, for $j = 1, \dots, N$. As it has been shown in [1], this yields the click counting distribution for k coincidence clicks in Eq. (1) via

$$c_k(\alpha) = \sum_{k_1 + \dots + k_N = k} c_{k_1, \dots, k_N}. \quad (4)$$

Note that $:e^{-\eta(\hat{n} + \mu|\alpha|^2)/N}$ is the measurement operator for the case that no click is recorded in a given bin.

Now assume that we have $N = q\tilde{N}$ for positive integers $q > 1$ and \tilde{N} . We want to infer the click statistics for the smaller number of bins, \tilde{N} . Thus, we cluster q bins into a single one and define that a click is recorded in a cluster if any of the included bins detects a click, i.e.,

$$\tilde{k}_j = \begin{cases} 0 & \text{for } k_{q(j-1)+1} = \dots = k_{q(j-1)+q} = 0, \\ 1 & \text{otherwise,} \end{cases} \quad (5)$$

* martin.bohmann@uni-rostock.de

for $j = 1, \dots, \tilde{N}$. Consequently, we get the coincidence statistics for the \tilde{N} clusters as

$$\tilde{c}_{\tilde{k}_1, \dots, \tilde{k}_{\tilde{N}}} = \left\langle : \prod_{\tilde{j}=1}^{\tilde{N}} \left[\left(e^{-\eta(\tilde{n} + \mu|\alpha|^2)/N} \right)^q \right]^{1-\tilde{k}_{\tilde{j}}} \right. \\ \left. \times \prod_{\tilde{j}=1}^{\tilde{N}} \left[\hat{1} - \left(e^{-\eta(\tilde{n} + \mu|\alpha|^2)/N} \right)^q \right]^{\tilde{k}_{\tilde{j}}} : \right\rangle_{\hat{\rho}_\alpha} \quad (6)$$

because the measurement operator that no click is recorded in a cluster is given by $: (e^{-\eta(\tilde{n} + \mu|\alpha|^2)/N})^q := : e^{-\eta(\tilde{n} + \mu|\alpha|^2)/\tilde{N}} :$, using $q/N = 1/\tilde{N}$ and with the same detection efficiency η . Therefore, the click counting statistics for the case that \tilde{k} out of \tilde{N} clusters record a click ($0 \leq \tilde{k} \leq \tilde{N}$) is given by

$$\tilde{c}_{\tilde{k}}(\alpha) = \sum_{\tilde{k}_1 + \dots + \tilde{k}_{\tilde{N}} = \tilde{k}} c_{\tilde{k}_1, \dots, \tilde{k}_{\tilde{N}}}, \quad (7)$$

which takes the same form as given in Eq. (1) when replacing N with \tilde{N} , similarly to the result in Ref. [1]. Therefore, clustering enables us to directly infer the click counting statistics for \tilde{N} detection bins from the click counting statistics for N detection bins if $\tilde{N} = N/q$.

II. MODEL OF THE GENERATED STATE

A. Exact P_N for relevant states

We can evaluate the phase-space function in Eq. (1) of the Letter, $P_N(\alpha; x) = \sum_{k=0}^N [(x-2)/x]^k c_k(\alpha)$. For example, a coherent signal state $|\beta\rangle$ results in

$$P_N^{(\beta)}(\alpha; x) = \left[\frac{x-2}{x} \left(1 - e^{-\nu(\alpha)} e^{-\eta|\alpha-\beta|^2/N} \right) \right. \\ \left. + e^{-\nu(\alpha)} e^{-\eta|\alpha-\beta|^2/N} \right]^N. \quad (8)$$

From this expression we can directly see that $P_N^{(\beta)}(\alpha; x)$ is nonnegative for any nonzero x and even N . The same holds true for any convex combination of coherent states and, thus, for any classical state [3]. Hence, in order to certify nonclassicality, it is sufficient to find an arbitrary real value $x \neq 0$ for which the corresponding $P_N(\alpha; x)$ is negative for at least one α . In particular, the x value does not necessarily need to correspond to a typical s value of any s -parametrized phase-space function, for which the restrictions $x = \eta(1-s)$ and $-1 \leq s \leq 1$ apply.

Further, based on the coherent state representation $|\beta\rangle = \hat{D}(\beta)|0\rangle = \exp(-|\beta|^2/2) \exp(\beta \hat{a}^\dagger)|0\rangle$, where \hat{a}^\dagger is the creation operator of the signal field, we can write photon-number states $|n\rangle = \hat{a}^{\dagger n}|0\rangle/\sqrt{n!}$ in the form

$$|n\rangle\langle n| = \frac{1}{n!} \partial_\beta^n \partial_{\beta^*}^n e^{|\beta|^2} |\beta\rangle\langle\beta| \Big|_{\beta=0}. \quad (9)$$

This allows us to write the click-counting phase-space functions for arbitrary photon-number contributions as the algebraic expression

$$P_N^{(n)}(\alpha; x) = \frac{1}{n!} \partial_\beta^n \partial_{\beta^*}^n e^{|\beta|^2} P_N^{(\beta)}(\alpha; x) \Big|_{\beta=0}. \quad (10)$$

B. Heralded single-photon states

In the ideal case, the type II parametric down-conversion source generates a two-mode squeezed vacuum. Assuming no phase stability between the signal and idler mode, we obtain a phase-randomized version of this state,

$$\hat{\rho}_{\text{PDC}} = (1-p) \sum_{n=0}^{\infty} p^n |n, n\rangle\langle n, n|, \quad (11)$$

with $0 < p < 1$. p is related to the squeezing parameter ξ of the two-mode squeezed-vacuum state, $|\xi| = \text{artanh}(\sqrt{p}) = \ln[(1+\sqrt{p})/(1-\sqrt{p})]/2$. Note that the state is symmetric in the two modes, signal and idler.

By performing a measurements in one of the modes, i.e., heralding, we generate the single-mode signal light. The measurement in the idler mode is also done with a click counter (here, a time-bin multiplexing detector). When conditioning to r clicks, the theory for this process [5] yields

$$\hat{\rho}_r = \mathcal{N}(1-p) \sum_{n=0}^{\infty} p^n \frac{N_h!}{(N_h-r)!} \\ \times \sum_{l=0}^n \binom{n}{l} (1-\eta_h)^l \left(\frac{\eta_h}{N_h} \right)^{n-l} \left\{ \begin{matrix} n-l \\ r \end{matrix} \right\} |n\rangle\langle n|, \quad (12)$$

where $\left\{ \begin{matrix} n-l \\ r \end{matrix} \right\}$ is the Stirling number of the second kind [6] and \mathcal{N} is a normalization constant. In addition, N_h and η_h define the number of time-bins and the quantum efficiency of the heralding time-bin multiplexing detector, respectively. In the case $r=1$, we obtain the standard approach to herald a single photons from photon-pair sources. We emphasize that our model accounts for the unavoidable imperfections of the heralding process by considering higher photon-number contributions, $n > r$.

The number of detection bins of the heralding detector is $N_h = 8$. From the fit of the model to the experimental data, we obtain the value $p = 0.09$ and an overall detection efficiency for the idler mode of $\eta_h = 12\%$. This results in the estimated fidelity of the one-click heralded state with a single-photon of $\langle 1|\hat{\rho}_1|1\rangle = 85\%$.

After the heralding process, the signal state is displaced at the unbalanced beam splitter. The superimposition with the weak coherent state $|\alpha\rangle$ leads to a displacement of the photon-number states in Eq. (12), i.e., each component $|n\rangle\langle n|$ is mapped to $\hat{D}(\alpha)|n\rangle\langle n|\hat{D}^\dagger(\alpha)$.

In Fig. 2 (left plot), we show P_N for $x = \eta$ for the best fit of the theoretically modeled state, which includes the



FIG. 2. Left: The theory fit (including all imperfections) of the full phase-space distribution $P_{N=8}(\alpha)$ corresponding to the data sampled for Fig. 4 (left) in the Letter. Right: In comparison, the theoretical prediction of the Wigner function $W(\alpha)$ for this state, which is nonnegative.

imperfections of the heralding of single photons, such as losses, mode mismatch, and higher photon-number contributions. For comparison, we get a nonnegative Wigner function (Fig. 2, right plot) for this state and the same

detection losses. Note that the high losses do not allow for observing the central dip, characteristic for single photons, in the Wigner function because of the high Gaussian vacuum contribution.

-
- [1] J. Sperling, W. Vogel, and G. S. Agarwal, True photo-counting statistics of multiple on-off detectors, *Phys. Rev. A* **85**, 023820 (2012).
 - [2] T. Lipfert, J. Sperling, and W. Vogel, Homodyne detection with on-off detector systems, *Phys. Rev. A* **92**, 053835 (2015).
 - [3] A. Luis, J. Sperling, and W. Vogel, Nonclassicality Phase-Space Functions: More Insight with Fewer Detectors, *Phys. Rev. Lett.* **114**, 103602 (2015).
 - [4] M. Bohmann, R. Kruse, J. Sperling, C. Silberhorn, and W. Vogel, Direct calibration of click-counting detectors, *Phys. Rev. A* **95**, 033806 (2017).
 - [5] J. Sperling, W. Vogel, and G. S. Agarwal, Quantum state engineering by click counting, *Phys. Rev. A* **89**, 043829 (2014).
 - [6] F. M. Miatto, A. Safari, and R. W. Boyd, Theory of multiplexed photon number discrimination, [arXiv:1601.05831](https://arxiv.org/abs/1601.05831).